

1 **Environmental Stability of Enveloped Viruses is Impacted by the Initial Volume and**  
2 **Evaporation Kinetics of Droplets**

3 Andrea J. French<sup>1\*</sup>, Alexandra K. Longest<sup>2\*</sup>, Jin Pan<sup>2</sup>, Peter J. Vikesland<sup>2</sup>, Nisha K. Duggal<sup>3</sup>,  
4 Seema S. Lakdawala<sup>1,4+</sup>, Linsey C. Marr<sup>2+</sup>

5

6 <sup>1</sup>Department of Microbiology & Molecular Genetics, University of Pittsburgh School of Medicine,  
7 Pittsburgh, PA

8 <sup>2</sup>Department of Civil and Environmental Engineering, Virginia Tech, Blacksburg, VA

9 <sup>3</sup>Department of Biomedical Sciences and Pathobiology, Virginia-Maryland College of Veterinary  
10 Medicine, Virginia Tech, Blacksburg, VA

11 <sup>4</sup>Center for Vaccine Research, University of Pittsburgh School of Medicine, Pittsburgh, PA

12 \*Authors contributed equally to this work

13 <sup>+</sup>Direct correspondence to [lakdawala@pitt.edu](mailto:lakdawala@pitt.edu) (SSL) and [lmarr@vt.edu](mailto:lmarr@vt.edu) (LCM)

14

15 **Keywords:** influenza, SARS-CoV-2, survival, stability, persistence, droplets, volume, size

16

17 **Running Title:** Respiratory virus stability in large & small droplets

18 **Abstract**

19 Efficient spread of respiratory viruses requires the virus to maintain infectivity in the  
20 environment. Environmental stability of viruses can be influenced by many factors, including  
21 temperature and humidity. Our study measured the impact of initial droplet volume (50, 5, and 1  
22  $\mu\text{L}$ ) and relative humidity (RH: 40%, 65%, and 85%) on the stability of influenza A virus,  
23 bacteriophage, Phi6, a common surrogate for enveloped viruses, and SARS-CoV-2 under a  
24 limited set of conditions. Our data suggest that the drying time required for the droplets to reach  
25 quasi-equilibrium (i.e. a plateau in mass) varied with RH and initial droplet volume. The  
26 macroscale physical characteristics of the droplets at quasi-equilibrium varied with RH but not  
27 with initial droplet volume. We observed more rapid virus decay when the droplets were still wet  
28 and undergoing evaporation, and slower decay after the droplets had dried. Initial droplet  
29 volume had a major effect on virus viability over the first few hours; whereby the decay rate of  
30 influenza virus was faster in smaller droplets. In general, influenza virus and SARS-CoV-2  
31 decayed similarly. Overall, this study suggests that virus decay in media is closely correlated  
32 with the extent of droplet evaporation, which is controlled by RH. Taken together, these data  
33 suggest that decay of different viruses is more similar at higher RH and in smaller droplets and  
34 is distinct at lower RH and in larger droplets. Importantly, accurate assessment of transmission  
35 risk requires use of physiologically relevant droplet volumes and careful consideration of the use  
36 of surrogates.

37

38 **Funding:** National Institute of Allergy and Infectious Diseases, National Institute of Neurological  
39 Disorders and Stroke, National Institutes of Health; Department of Health and Human Services;  
40 Flu Lab.

41

42 **Importance**

43 During the COVID-19 pandemic, policy decisions were being driven by virus stability  
44 experiments involving SARS-CoV-2 applied to surfaces in large droplets at various humidity  
45 conditions. The results of our study indicate that determination of half-lives for emerging  
46 pathogens in large droplets likely over-estimates transmission risk for contaminated surfaces, as  
47 occurred during the COVID-19 pandemic. Our study implicates the need for the use of  
48 physiologically relevant droplet sizes with use of relevant surrogates in addition to what is  
49 already known about the importance of physiologically relevant media for risk assessment of  
50 future emerging pathogens.

51

## 52 **Introduction**

53 Respiratory viruses, such as influenza A virus and SARS-CoV-2, contribute to high morbidity  
54 and mortality. These viruses must remain infectious in the environment for transmission to the  
55 next host to succeed. Understanding how environmental, host, and virus factors impact the  
56 stability of expelled virus will lead to a better assessment of virus transmission risk and ways to  
57 reduce it.

58 Many factors can impact virus stability in the environment, including virion structure,  
59 temperature, relative humidity (RH), droplet composition, solute concentration, and fomite  
60 surface material.<sup>1-5</sup> However, the relationship between droplet size and virus stability is not well  
61 understood, even though droplet size plays an important role in virus transmission by governing  
62 the distance traveled by respiratory expulsions.<sup>6</sup> Smaller droplets, or aerosols, can travel further  
63 from the infected host, while larger droplets settle to the ground more quickly due to their  
64 increased mass.<sup>6</sup> Droplet or aerosol size can also be a determinant of host infection site, as  
65 those smaller than 10  $\mu\text{m}$  in diameter are more likely to deposit deeper in the respiratory tract.<sup>7</sup>  
66 Understanding how droplet volume affects virus stability is critical to mitigating transmission of  
67 respiratory viruses such as influenza virus and coronaviruses.

68 Studies measuring virus stability in the environment typically use one of two methods to produce  
69 the inoculum: nebulizers to produce aerosols, or pipettes to create droplets of volumes ranging  
70 from 5 to 50  $\mu\text{L}$ . While large droplets are commonly used to assess environmental virus stability,  
71 they do not mimic a physiological volume of a droplet created by an expulsion. The vast majority  
72 of expelled droplets from the respiratory tract are less than 0.5  $\mu\text{L}$  in volume (approximately 1  
73 mm in diameter for a sphere). In contrast, a droplet of 50  $\mu\text{L}$  (approximately 4.6 mm in diameter  
74 if spherical) is about 5 times larger and 100 times greater in volume.<sup>8</sup> Studies measuring the  
75 stability of SARS-CoV-2 on surfaces have examined the virus in 5,<sup>9</sup> 10,<sup>10</sup> 20,<sup>11</sup> or 50  $\mu\text{L}$  droplets,  
76<sup>2,3,12</sup> which are much larger than naturally expelled droplets. These initial studies into SARS-  
77 CoV-2 stability were used widely to assert the importance of fomite transmission and set  
78 policies. However, little work has been done to understand whether virus decay in large droplets  
79 is representative of decay in smaller, more physiologically relevant droplet volumes.

80 This study primarily used the 2009 pandemic influenza H1N1 virus (H1N1pdm09,  
81 A/CA/07/2009) and bacteriophage Phi6, a commonly used virus surrogate, to examine  
82 environmental stability of enveloped viruses in three different droplet volumes at three different  
83 RHs over time. Specifically, we measured the viability of each virus in 50, 5, and 1  $\mu\text{L}$  droplets  
84 on surfaces over time at 40%, 65%, and 85% RH. We observed that virus within smaller  
85 droplets decays quickly regardless of RH, while virus decay occurs more slowly in larger  
86 droplets. We also explored droplet evaporation rates and found that virus decay is closely  
87 correlated with the extent of evaporation, which is likely a proxy for solute concentrations in the  
88 droplet. Additionally, limited experiments with SARS-CoV-2 showed that influenza virus decayed  
89 similarly to SARS-CoV-2 at an intermediate 55-60% RH in 50, 5, and 1  $\mu\text{L}$  droplets. Overall, our  
90 results suggest that virus stability studies should use smaller, more physiologically relevant  
91 droplet volumes and should recognize the limitations of surrogate viruses.

## 92 **Results**

### 93 **Relative humidity alters morphology of evaporating droplets and drying kinetics**

94 We expect the physical and chemical characteristics of droplets to influence decay of viruses  
95 within each droplet. Some of these characteristics may be reflected in the morphology of  
96 droplets after they have dried.<sup>5</sup> Furthermore, fluid dynamics within droplets could lead to  
97 increased aggregation of virus, which can enhance virus stability.<sup>13,14</sup> We investigated whether

98 droplet morphology and drying pattern at 24 hours differed between 1x50, 5x5, and 10x1  $\mu\text{L}$   
99 droplets (i.e., one droplet of volume 50  $\mu\text{L}$ , five droplets of volume 5  $\mu\text{L}$ , ten droplets of volume 1  
100  $\mu\text{L}$ ). Droplets of Dulbecco's Modified Eagle Medium (DMEM) were placed on polystyrene plastic  
101 and incubated at 40%, 65%, or 85% RH for 24 hours (Figure 1). These RH were selected to  
102 match values in other published work.<sup>2</sup> At 40% RH, feather-like crystals grew throughout the  
103 dried droplet. At 65% RH, we observed fewer distinct crystals in the interior of the dried droplet.  
104 At 85% RH, the droplets retained a sheen, and crystallization did not occur. The effect of RH on  
105 dried droplet morphology was independent of initial droplet volume. The morphology of droplets  
106 containing virus was the same as that of droplets consisting of media alone (data not shown).  
107 Our results show that the droplet drying pattern at 24 hours depends on RH but not initial  
108 droplet volume, so any differences in viral decay by droplet size would not be due to final  
109 physico-chemical differences.

110 Evaporation leads to the concentration of solutes, which can influence virus stability in  
111 droplets.<sup>15</sup> To investigate the drying kinetics, we recorded the mass of droplets over time for 24  
112 hours at ambient temperature and the same three RHs. At all RHs, the droplets lost mass  
113 linearly over time before reaching a plateau, referred to as a quasi-equilibrium (Supplemental  
114 Figure 1, Supplemental Table 1).<sup>2</sup> We defined this state as quasi-equilibrium because it is likely  
115 that very slow evaporation continues over a much longer time scale until complete dryness  
116 occurs, or until a crust or shell forms that blocks further water loss. To simplify discussion, we  
117 refer to the time period before this as the “wet” phase and the period after this as the “dry”  
118 phase. Evaporation was faster for smaller droplets and lower RH (Supplemental Table 2). The  
119 time to reach quasi-equilibrium ranged from 0.5 hours for 1  $\mu\text{L}$  droplets at 40% RH to 11 hours  
120 for 50  $\mu\text{L}$  droplets at 85% RH. These data indicate that droplets of different volumes undergo  
121 different drying kinetics. If the kinetics of drying affect virus stability, then it could differ by initial  
122 droplet volume.

123

#### 124 **Virus decay is more sensitive to relative humidity in large droplets.**

125 To directly examine how RH and droplet volume impact virus stability, we applied virus in  
126 droplets of different volumes to a polystyrene surface and quantified recovery of infectious virus  
127 over time.<sup>16</sup> We compared decay of H1N1pdm09 and Phi6 at in 1x50  $\mu\text{L}$ , 5x5  $\mu\text{L}$ , and 10x1  $\mu\text{L}$   
128 droplets at 40%, 65%, and 85% RH (Figure 2). In 50  $\mu\text{L}$  droplets, Phi6 decayed fastest at 40%  
129 RH and slowest at 85% RH (Figure 2A). The impact of RH on the decay of H1N1pdm09 in 50  
130  $\mu\text{L}$  droplets over the first 8 hours was similar as for Phi6 but less pronounced, with the fastest  
131 decay occurring at 40% RH (Figure 2B). Decay of H1N1pdm09 in the 50  $\mu\text{L}$  droplet was first  
132 detected at 4 hours at 40% RH, 8 hours at 65% RH, and 24 hours at 85% RH, indicating that  
133 early virus decay was inversely related to RH (i.e., faster decay at lower RH) (Supplemental  
134 Table 4). Decay of Phi6 in 5  $\mu\text{L}$  droplets differed by RH only at 1 hour, when decay at 40% was  
135 greater than at 85%. In 1  $\mu\text{L}$  droplets, decay differed between 40 minutes and 4 hours by RH  
136 but was not significantly different at 8 hours and afterward (Figure 2A). H1N1pdm09 in 1  $\mu\text{L}$  and  
137 5  $\mu\text{L}$  droplets decayed at a similar rate regardless of RH (Figure 2B). Phi6 was more unstable  
138 after drying at the intermediate RHs, whereas H1N1pdm09 tended to be more stable. This  
139 accounts for differences in decay at the smaller droplet sizes. These findings show that the  
140 impact of RH on virus decay in droplets depends on the virus and the initial volume of the  
141 droplets.

142

#### 143 **Virus decay rates are faster during the wet phase and depend on droplet volume and 144 virus.**

145 The pattern of decay for Phi6 and H1N1pdm09 appeared distinct for different droplet volumes.  
146 This led us to investigate whether evaporation rate impacts virus decay and whether different  
147 viruses behave similarly across different droplet volumes. Virus decay often follows first-order  
148 kinetics.<sup>17</sup> Following a previously developed mechanistic model of virus inactivation in droplets,  
149 we fit an exponential decay model to virus titers in droplets during the wet phase (prior to quasi-  
150 equilibrium) and a separate curve during the dry phase to create a biphasic model (Figures 3  
151 and 4, Table 1).<sup>4</sup> The model accounts for changing solute concentrations in the droplets as they  
152 evaporate during the wet phase.<sup>2</sup> In most cases, decay was faster in the wet phase than in the  
153 dry phase. Figure 3 shows viability as a function of time for two conditions: 5x5  $\mu$ L droplets at  
154 40% RH (Figure 3A-B) and 10x1  $\mu$ L droplets at 65% RH (Figure 3C-D). The insets show the  
155 detail during the first 1.5 hours (Figure 3B, D), when the droplets transitioned from wet to dry.  
156 Similar trends are evident in most of the nine combinations of initial volume and RH for both  
157 viruses (Figure 4 and Table 1).

158 Among the 12 combinations of RH and initial droplet volume for which the decay rate constant  
159 could be compared between the wet phase and dry phase, it was larger in magnitude during the  
160 wet phase than during the dry phase in most cases and significantly larger in 3 of 12 of these  
161 cases (Table 1, Supplemental Table 5): Phi6 in 5x5  $\mu$ L droplets at 40% RH (Figure 3A),  
162 H1N1pdm09 in 5x5  $\mu$ L droplets at 40% RH (Figure 3A), and Phi6 in 5x5  $\mu$ L droplets at 65% RH  
163 (Figure 4B). Because there were only two time points during the wet phase for the 10x1  $\mu$ L  
164 droplets at 40% RH and only one or two time points during the dry phase for 1x50  $\mu$ L droplets at  
165 65% and 85% RH, it was not possible to compare decay rates for these conditions (Table 1)

166 Comparing decay rates as a function of droplet size, we found that for H1N1pdm09 at a given  
167 RH and phase, the decay rate constant was often higher in smaller droplets compared to larger  
168 ones, mainly in the wet phase, although differences were only significant at 40% RH between  
169 50 and 5  $\mu$ L droplets in the wet phase. For Phi6, there were no apparent trends in the decay  
170 rate as a function of initial droplet volume.

171 Comparing decay rates by virus, we found that the decay rate constant was significantly higher  
172 for Phi6 than H1N1pdm09 in two cases during the wet phase and was significantly different in  
173 two cases—higher for H1N1pdm09 in both cases—during the dry phase (Figure 4, Table 1).  
174 Significant differences were not observed in the 1  $\mu$ L droplets. These results indicate that  
175 different enveloped RNA viruses may decay differently.

176

## 177 **H1N1pdm09 decays similarly to SARS-CoV-2 at intermediate RH.**

178 Given the observed differences in the decay rate constants of H1N1pdm09 and Phi6 (Figure 4,  
179 Table 1), we further investigated how the stability of these two viruses compared to that of  
180 SARS-CoV-2 using both original and previously published data.<sup>2</sup> To determine whether these  
181 viruses undergo similar patterns of decay at 40%, 65%, and 85% RH, we compared our results  
182 for H1N1pdm09 and Phi6 in 50  $\mu$ L droplets to published results for SARS-CoV-2 (Figure 5, A-C,  
183 Supplemental Table 6).<sup>2</sup> There were significant differences for each pairwise comparison of the  
184 decay of H1N1pdm09, Phi6, and SARS-CoV-2 at 40% RH at 4 and 8 hours. SARS-CoV-2 was  
185 most stable, followed by H1N1pdm09 and then Phi6 (Figure 5A). At 65% RH, there were fewer  
186 differences: only Phi6 was significantly different (less stable) from H1N1pdm09 and SARS-CoV-  
187 2 again at 4 and 8 hours (Figure 5B). At 85% RH, there were no significant differences for the  
188 decay of any pairwise comparison (Figure 5C). Significance at 24 hours was not assessed due  
189 to virus decay reaching the limit of detection for at least one of the viruses tested. This suggests  
190 that in large 50  $\mu$ L droplets, virus-specific differences are greater at lower RH.

191 To understand the role of droplet volume on decay of different enveloped respiratory viruses, we  
192 assessed titers of SARS-CoV-2 and H1N1pdm09 in 1x50  $\mu$ L, 5x5  $\mu$ L, and 10x1  $\mu$ L droplets at  
193 55% and 60% RH, respectively. Due to technical limitations, we were not able to test the exact  
194 same RH, but we consider these conditions to be similar. SARS-CoV-2 stability in 1x50  $\mu$ L, 5x5  
195  $\mu$ L, and 10x1  $\mu$ L droplets at 55% RH was similar to that of H1N1pdm09 at 60% RH, except for  
196 the 50  $\mu$ L droplets at 4 hours (Figure 6, A-C, Supplemental Table 7). While decay of SARS-  
197 CoV-2 at 24 hours appeared to be greater, H1N1pdm09 had reached the maximum decay  
198 corresponding to the limit of detection. After 8 hours, decay was greatest in the 1  $\mu$ L droplets  
199 and least in the 50  $\mu$ L droplets. Taken together with Figure 5, these results show that SARS-  
200 CoV-2 and H1N1pdm09 decay similarly at intermediate RH and that differences in virus decay  
201 are evident in larger droplets.

202

## 203 Discussion

204 The studies detailed here characterize the interplay of droplet volume and RH on the stability of  
205 three enveloped RNA viruses: Phi6, H1N1pdm09, and SARS-CoV-2. Our results showed that  
206 RH has a greater impact on viral decay in large 50  $\mu$ L droplets than in small 1  $\mu$ L droplets, that  
207 decay rates during the wet phase are greater than or similar to decay rates during the dry phase  
208 regardless of droplet size and RH, and that differences in virus decay are more common in 50  
209  $\mu$ L droplets than in 1  $\mu$ L droplets and at low RH.

210 Our results raise questions about the application of prior studies on stability of viruses that  
211 employ large droplet volumes to real-world transmission. For example, one study derived a half-  
212 life (~0.3-log decay) of 6.8 hours for SARS-CoV-2 in 50  $\mu$ L droplets on polypropylene plastic.<sup>3</sup>  
213 Another used 5  $\mu$ L droplets to evaluate the lifetime of SARS-CoV-2 on different materials, and  
214 reported 0.5-log decay in 3 hours and 1.1-log decay in 6 hours on plastic, similar to the results  
215 shown here (Figure 6B).<sup>9</sup> The conclusions of studies might have differed had they used smaller,  
216 more physiologically relevant droplet volumes. In our study, after 4 hours, we observed no  
217 significant decay in 50  $\mu$ L droplets, ~1-log decay in 5  $\mu$ L droplets, and ~1.5-log decay in 1  $\mu$ L  
218 droplets at 55-60% RH. Over longer time periods, results converged; we observed at least 3-log  
219 decay in all three droplet volumes after 24 hours. These differences are likely controlled by  
220 physical and chemical properties of the droplets as they undergo evaporation at different rates,  
221 depending on their initial volume and ambient humidity.

222 We have attempted to study viruses in a more realistic droplet volume compared to those used  
223 in past research, but even a 1  $\mu$ L droplet is at the extremely large end of the range of droplet  
224 volumes observed in respiratory emissions. During talking, coughing, and sneezing, droplets of  
225 this size are emitted in much lower numbers, by many orders of magnitude, compared to those  
226 that behave as aerosols.<sup>6</sup> While we observed differences between 50  $\mu$ L and 1  $\mu$ L droplets in  
227 this study, previous work has shown that virus in 1  $\mu$ L droplets undergoes similar decay to that  
228 in aerosols at 23% to 98% RH and 22°C.<sup>18</sup> New techniques are needed to study smaller droplet  
229 volumes on surfaces.

230 Our results also suggest caution in the use of surrogates to study the stability of pathogenic  
231 viruses and their potential for transmission.<sup>19</sup> Surrogates can be useful for evaluating sampling  
232 and analysis methods, studying physico-chemical processes such as mechanisms of decay and  
233 transport in complex media, or eliciting trends in survival in complex media.<sup>1,18,20,21</sup> However, we  
234 should be cautious about extrapolating survival times from surrogates to other viruses. In the  
235 present study, we found that Phi6 decayed more quickly than did H1N1pdm09 and SARS-CoV-2  
236 under our experimental conditions. Relying on only Phi6 data could lead to incorrect, and  
237 potentially hazardous, conclusions about pathogenic viruses. Strain selection should also be

238 considered when using influenza virus, as previous work has shown that avian influenza viruses  
239 undergo more rapid decay compared to human influenza viruses.<sup>22</sup> Decay of enveloped viruses  
240 is likely dependent upon many complex interactions of media components with the viral  
241 glycoprotein and changes to it during and after drying. Thus variations in glycoprotein content  
242 and density per virus family or strain likely influence the stability within droplets. On the other  
243 hand, H1N1pdm09 decayed more similarly to SARS-CoV-2 and could be useful surrogate to  
244 extrapolate the latter's persistence in more physiologically relevant conditions.

245 A major limitation of this study is that we used culture medium, DMEM, that may not be  
246 representative of real respiratory fluid. We selected this medium for the purpose of comparing  
247 results with prior studies of SARS-CoV-2 in DMEM.<sup>2,3</sup> Prior studies have shown that virus  
248 survival in droplets, including suspended aerosols, is strongly dependent on the chemical  
249 composition of the suspending medium.<sup>1,20,23</sup> In particular, we have previously shown that  
250 H1N1pdm09 in aerosols and 1  $\mu$ L droplets survived better when the suspending medium was  
251 supplemented with extracellular material from human bronchial epithelial cells.<sup>1</sup> Further studies  
252 will be required to characterize whether extracellular material from airway cells affects the decay  
253 patterns observed in this study.

254 Extrapolating our results to smaller droplet sizes and combining them with the findings of other  
255 studies may provide mechanistic insight into the dynamics of virus inactivation in droplets and  
256 aerosols. The biphasic virus decay that is readily observed in droplets likely occurs in aerosols,  
257 too, as shown in published work and a preprint.<sup>2,9,24,25</sup> While a droplet/aerosol is wet and  
258 evaporation is still occurring, the virus is subject to a faster decay rate than after the  
259 droplet/aerosol reaches a solid or semi-solid state at quasi-equilibrium,<sup>5</sup> as we also observed for  
260 all droplet sizes tested. At the point of efflorescence (the crystallization of salts as water  
261 evaporates), if it occurs, there appears to be a rapid loss in infectivity. With aerosols, the first  
262 phase occurs quickly, within seconds, and further observations of decay are dominated by the  
263 quasi-equilibrium phase. Thus, the first phase of decay is important for transmission at close  
264 range, when exposure occurs within seconds, whereas both phases are important for  
265 transmission at farther range.

266 Although virus stability in droplets and aerosols appears to be a complex function of droplet  
267 size, composition, humidity, and other variables, mechanistically their role is to modulate the  
268 microenvironment surrounding a virion, as suggested in published work and a preprint.<sup>5,25,26</sup>  
269 Ultimately, molecular-scale interactions are what lead to virus inactivation. We combined results  
270 for all droplet sizes and all RHs and plotted virus decay as a function of extent of evaporation of  
271 a droplet, a proxy for its instantaneous physical and chemical characteristics, and found that the  
272 points appeared to converge more so than in Figures 2 and 4 (Supplemental Figure 2). The  
273 exact mechanisms of virus inactivation—the biochemical changes that occur—remain unknown  
274 and are ripe for further investigation.

275 Due to our findings on the sensitivity of virus persistence to both droplet volume and  
276 composition, we urge a shift toward the use of more realistic conditions in future studies. They  
277 should employ droplets as close in volume as possible to those released from the respiratory  
278 tract (sub-micron up to several hundred microns in diameter), and whose chemical composition  
279 closely mimics that of real respiratory fluid. These findings are critical for pandemic risk  
280 assessment of emerging pathogens and useful to improve public policy on optimal transmission  
281 mitigation strategies.

282

## 283 **Methods**

284 **Evaporation experiment**

285 Droplet mass was recorded every 10 minutes for up to 24 hours using a micro-balance.  
286 Experiments were performed in duplicate. Additional information can be found in the  
287 supplemental methods.

288 **Stability studies**

289 We measured virus stability for Phi6 and H1N1pdm09 in a humidity-controlled chamber  
290 (Electro-Tech Systems) at room temperature and three (40%, 65%, and 85%) or four RHs,  
291 respectively (40%, 60%, 65%, and 85%). A logger (HOBO UX100-011) placed inside the  
292 chamber recorded relative humidity and temperature. Droplets were pipetted onto 6-well  
293 polystyrene tissue culture-coated plates (Thermo Scientific) in technical duplicates. Droplets  
294 were resuspended at seven different time points (0 minutes, 20 minutes, 40 minutes, 1 hour, 4  
295 hours, 8 hours, and 24 hours), or four time points (1, 4, 8 and 24 hours) for the experiment at  
296 60% RH, using 500  $\mu$ L of DMEM containing 2% FBS, penicillin/streptomycin, and L-glutamine.

297 We measured the stability of SARS-CoV-2 in an airtight desiccator at room temperature and  
298 55% RH as described previously.<sup>18</sup> In short, we filled one polyethylene Petri dish with 10 to 20  
299 mL of saturated magnesium nitrate solution and placed it and a fan at the bottom of the  
300 desiccator to control the humidity. After RH equilibrium was reached, usually within 5-10  
301 minutes, we deposited droplets and later resuspended them as described previously. We  
302 measured virus titers by plaque assay on Vero cells. All collections were performed in technical  
303 duplicates and independent triplicates.

304 **Cells and viruses**

305 Information regarding virus growth and quantification can be found in the supplement.

306 **Modeling**

307 Virus decay calculations and modeling are described in the supplement.

308 **Role of the funding source**

309 The study sponsors had no role in the study design, data collection, data analysis, data  
310 interpretation, or writing of the report.

311

312 **Contributors**

313 SSL and LCM conceptualized and designed the study. NKD, SSL, and LCM supervised the  
314 study. AJF, AKL, and JP developed methodology, acquired data through plaque assays, and  
315 analyzed the data, and produced figures. PJV analyzed data on droplet characteristics. AJF and  
316 AKL wrote the first draft of the manuscript. All authors revised and edited the final version of the  
317 manuscript. All authors had access to all the data in the study and accept responsibility for the  
318 publication.

319 **Declaration of interests**

320 We declare no competing interests.

321 **Data sharing**

322 The data collected in this study are publicly available in the Virginia Tech Data Repository at  
323 <https://doi.org/10.7294/20134796>.

324 **Acknowledgements**

325 This work was supported by NIAID (CEIRS HHSN272201400007C, SSL and LCM), and in part  
326 with Federal funds from NIAID, NIH, and DHHS (CEIRR contract number 75N93021C00015,  
327 SSL). Additional funding was provided by Flu Lab (SSL and LCM), the Virginia Tech ICTAS  
328 Junior Faculty Award and NIH NINDS R01NS124204 (NKD). JF was supported by the  
329 University of Pittsburgh Training Program in Antimicrobial Resistance (T32AI138954). We thank  
330 Dr. Rachel Schwartz for critical review and feedback. We also thank Dr. Douglas Reed and his  
331 lab for allowing us access to the humidity cabinet used in these experiments.

332 **References**

333 1 Kormuth KA, Lin K, Prussin AJ, *et al.* Influenza virus infectivity is retained in  
334 aerosols and droplets independent of relative humidity. *Journal of Infectious*  
335 *Diseases* 2018; **218**: 739–747.

336 2 Morris DH, Yinda KC, Gamble A, *et al.* Mechanistic theory predicts the effects of  
337 temperature and humidity on inactivation of sars-cov-2 and other enveloped  
338 viruses. *Elife* 2021; **10**: e65902.

339 3 van Doremalen N, Bushmaker T, Morris DH, *et al.* Aerosol and surface stability of  
340 SARS-CoV-2 as compared with SARS-CoV-1. *NEJM* 2020; **382**: 1564–1567.

341 4 Firquet S, Beaujard S, Lobert P-E, *et al.* Survival of enveloped and non-enveloped  
342 viruses on inanimate surfaces. *Microbes and Environments* 2015; **30**: 140–144.

343 5 Huynh E, Olinger A, Woolley D, *et al.* Evidence for a semisolid phase state of  
344 aerosols and droplets relevant to the airborne and surface survival of pathogens.  
345 *Proc Natl Acad Sci U S A* 2022; **119**: e2109750119.

346 6 Bourouiba L. Fluid dynamics of respiratory infectious diseases. *Annual Review of*  
347 *Biomedical Engineering* 2021; **23**: 547–577.

348 7 Gralton J, Tovey E, McLaws ML, Rawlinson WD. The role of particle size in  
349 aerosolised pathogen transmission: A review. *Journal of Infection*. 2011; **62**: 1–13.

350 8 Johnson G, Kat D, Wan MP, *et al.* Modality of human expired aerosol size  
351 distributions. *Journal of Aerosol Science* 2011; **42**: 839–851.

352 9 Chin AWH, Chu JTS, Perera MRA, *et al.* Stability of SARS-CoV-2 in different  
353 environmental conditions. *The Lancet Microbe* 2020; **1**: e10.

354 10 Kasloff SB, Leung A, Strong JE, Funk D, Cutts T. Stability of SARS-CoV-2 on  
355 critical personal protective equipment. *Scientific Reports* 2021 11:1 2021; **11**: 1–7.

356 11 Newey CR, Olausson AT, Applegate A, Reid A-A, Robison RA, Grose JH.  
357 Presence and stability of SARS-CoV-2 on environmental currency and money  
358 cards in Utah reveals a lack of live virus. *PLOS ONE* 2022; **17**: e0263025.

359 12 Liu Y, Li T, Deng Y, *et al.* Stability of SARS-CoV-2 on environmental surfaces and  
360 in human excreta. *Journal of Hospital Infection* 2021; **107**: 105–107.

361 13 Gerba CP, Betancourt WQ. Viral aggregation: impact on virus behavior in the  
362 environment. *Environmental Science and Technology* 2017; **51**: 7318–7325.

363 14 Huang Q, Wang W, Vikesland PJ. Implications of the coffee-ring effect on virus  
364 infectivity. *Langmuir* 2021; **37**: 11260–11268.

365 15 Marr LC, Tang JW, Mullekom J van, Lakdawala SS. Mechanistic insights into the  
366 effect of humidity on airborne influenza virus survival, transmission and incidence.  
367 *Journal of the Royal Society Interface* 2019; **16**: 20180298.

368 16 Reed LJ, Muench H. A simple method of estimating fifty percent endpoints.  
369 *American Journal of Epidemiology* 1938; **27**: 493–497.

370 17 Hiatt CW. Kinetics of the inactivation of viruses. *Bacteriological Reviews* 1964; **28**:  
371 150–163.

372 18 Prussin AJ, Schwake DO, Lin K, Gallagher DL, Buttling L, Marr LC. Survival of the  
373 enveloped virus phi6 in droplets as a function of relative humidity, absolute  
374 humidity, and temperature. *Appl Environ Microbiol* 2018; **84**: e00551-18.

375 19 Verreault D, Moineau S, Duchaine C. Methods for sampling of airborne viruses.  
376 *Microbiology and Molecular Biology Reviews* 2008; **72**: 413–44.

377 20 Lin K, Schulte CR, Marr LC. Survival of MS2 and Φ6 viruses in droplets as a  
378 function of relative humidity, pH, and salt, protein, and surfactant concentrations.  
379 *PLOS ONE* 2020; **15**: e0243505.

380 21 Lin K, Marr LC. Aerosolization of ebola virus surrogates in wastewater systems.  
381 *Environmental Science and Technology* 2017; **51**: 2669–2675.

382 22 Kormuth KA, Lin K, Qian Z, Myerburg MM, Marr LC, Lakdawala SS. Environmental  
383 persistence of influenza viruses is dependent upon virus type and host origin.  
384 *mSphere* 2019; **4**: 1–14.

385 23 Yang W, Elankumaran S, Marr LC. Relationship between humidity and influenza A  
386 viability in droplets and implications for influenza's seasonality. *PLOS ONE* 2012;  
387 **7**: e46789.

388 24 Harper G. Airborne micro-organisms: survival tests with four viruses. *The Journal  
389 of Hygiene* 1961; **59**: 479–486.

390 25 [preprint] Oswin HP, Haddrill AE, Otero-Fernandez M, et al. The dynamics of  
391 SARS-CoV-2 infectivity with changes in aerosol microenvironment. *medRxiv* 2022;  
392 2022.01.08.22268944, <https://doi.org/10.1101/2022.01.08.22268944>.

393 26 Vejerano EP, Marr LC. Physico-chemical characteristics of evaporating respiratory  
394 fluid droplets. *Journal of The Royal Society Interface* 2018; **15**: 20170939.

395 27 Ramakrishnan MA. Determination of 50% endpoint titer using a simple formula.  
396 *World Journal of Virology* 2016; **5**: 85–86.

397 28 Daugelavičius R, Cvirkaitė V, Gaidelytė A, Bakienė E, Gabrėnaitė-Verkhovskaya  
398 R, Bamford DH. Penetration of enveloped double-stranded RNA bacteriophages  
399 φ13 and φ6 into *Pseudomonas syringae* cells. *Journal of Virology* 2005; **79**: 5017–  
400 5026.

401 29 Hawks SA, Prussin AJ, Kuchinsky SC, Pan J, Marr LC, Duggal NK. Infectious  
402 SARS-CoV-2 is emitted in aerosol particles. *mBio* 2021; **12**: e02527-21.

403

404

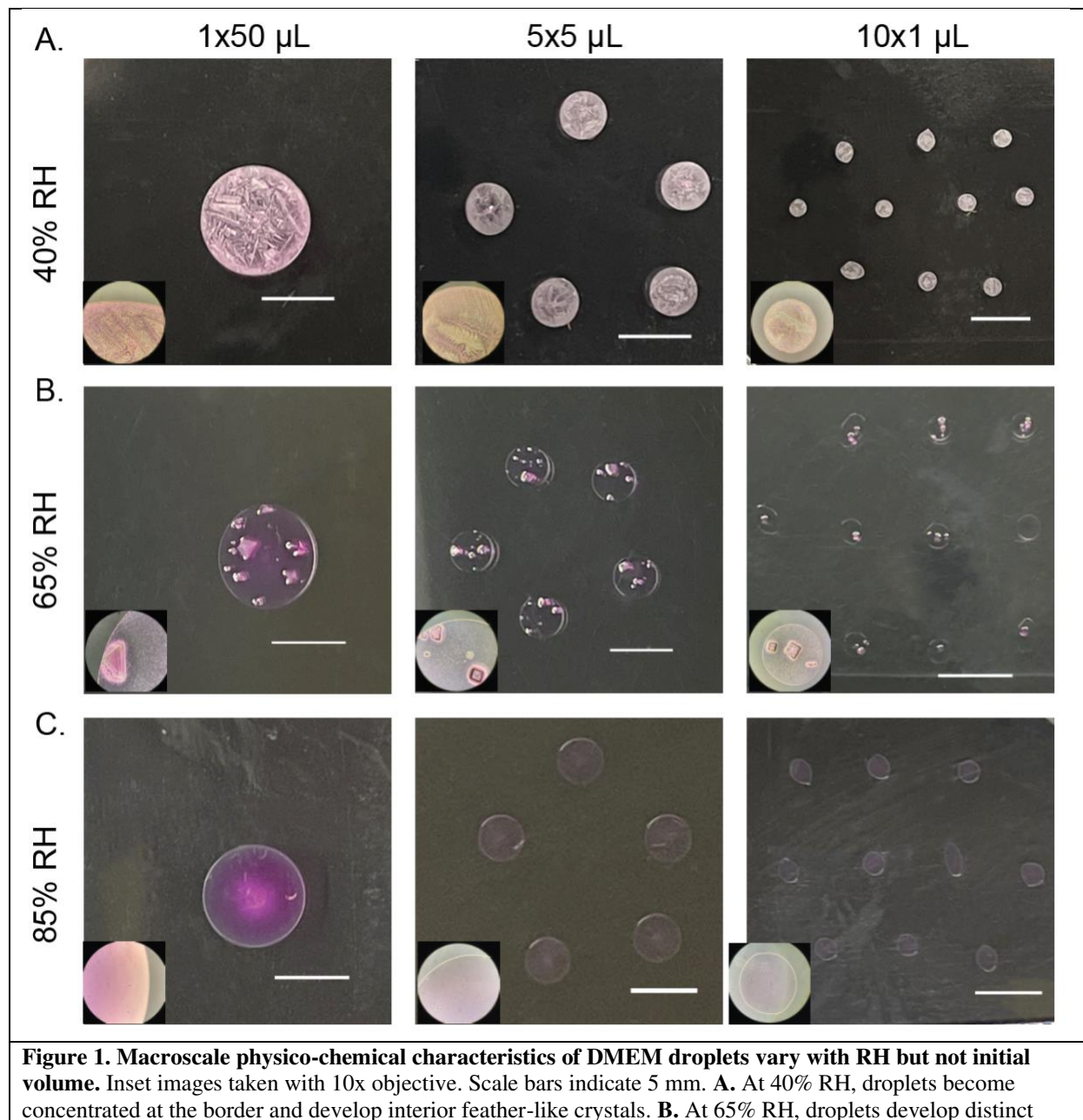


**Figure 1. Macroscale physico-chemical characteristics of DMEM droplets vary with RH but not initial volume.** Inset images taken with 10x objective. Scale bars indicate 5 mm. **A.** At 40% RH, droplets become concentrated at the border and develop interior feather-like crystals. **B.** At 65% RH, droplets develop distinct crystals within the interior. **C.** At 85% RH, droplets maintain moisture and do not crystallize.

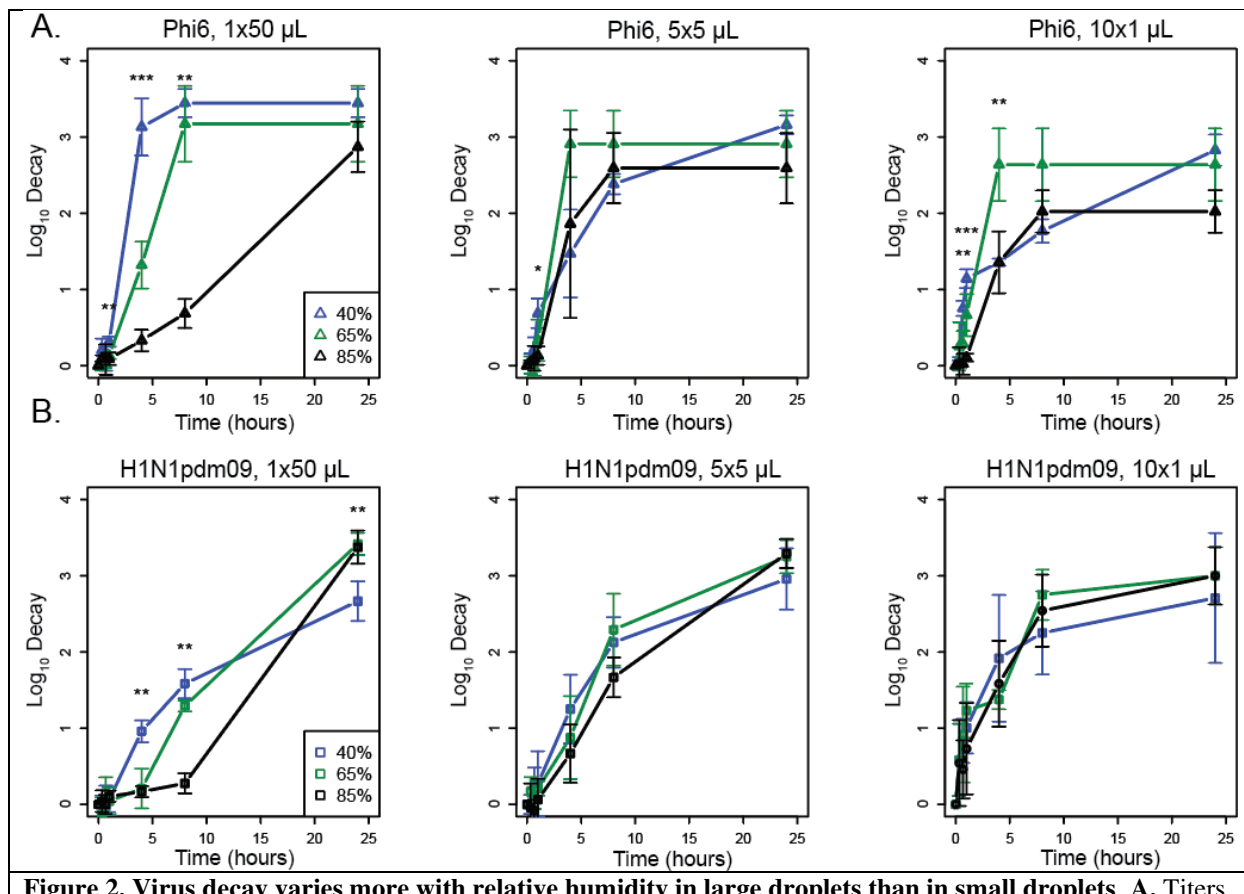


**Figure 2. Virus decay varies more with relative humidity in large droplets than in small droplets.** **A.** Titers of Phi6 in 1x50  $\mu\text{L}$ , 5x5  $\mu\text{L}$ , or 10x1  $\mu\text{L}$  droplets compared at 40%, 65%, and 85% RH in terms of  $\log_{10}$  decay. **B.** Titers of H1N1pdm09 in 1x50  $\mu\text{L}$ , 5x5  $\mu\text{L}$ , or 10x1  $\mu\text{L}$  droplets compared at 40%, 65%, and 85% RH in terms of  $\log_{10}$  decay. Error bars show standard deviation. Asterisks indicate significant differences between two or three RHs. For all graphs N=3 except at 1 hour where H1N1pdm09 N=6. One-way ANOVA tests were conducted between the RHs at each time point. A Tukey HSD test was conducted to determine between which RHs the significant differences ( $p < 0.05$ ) occurred. Statistical details can be found in Supplemental Table 3.

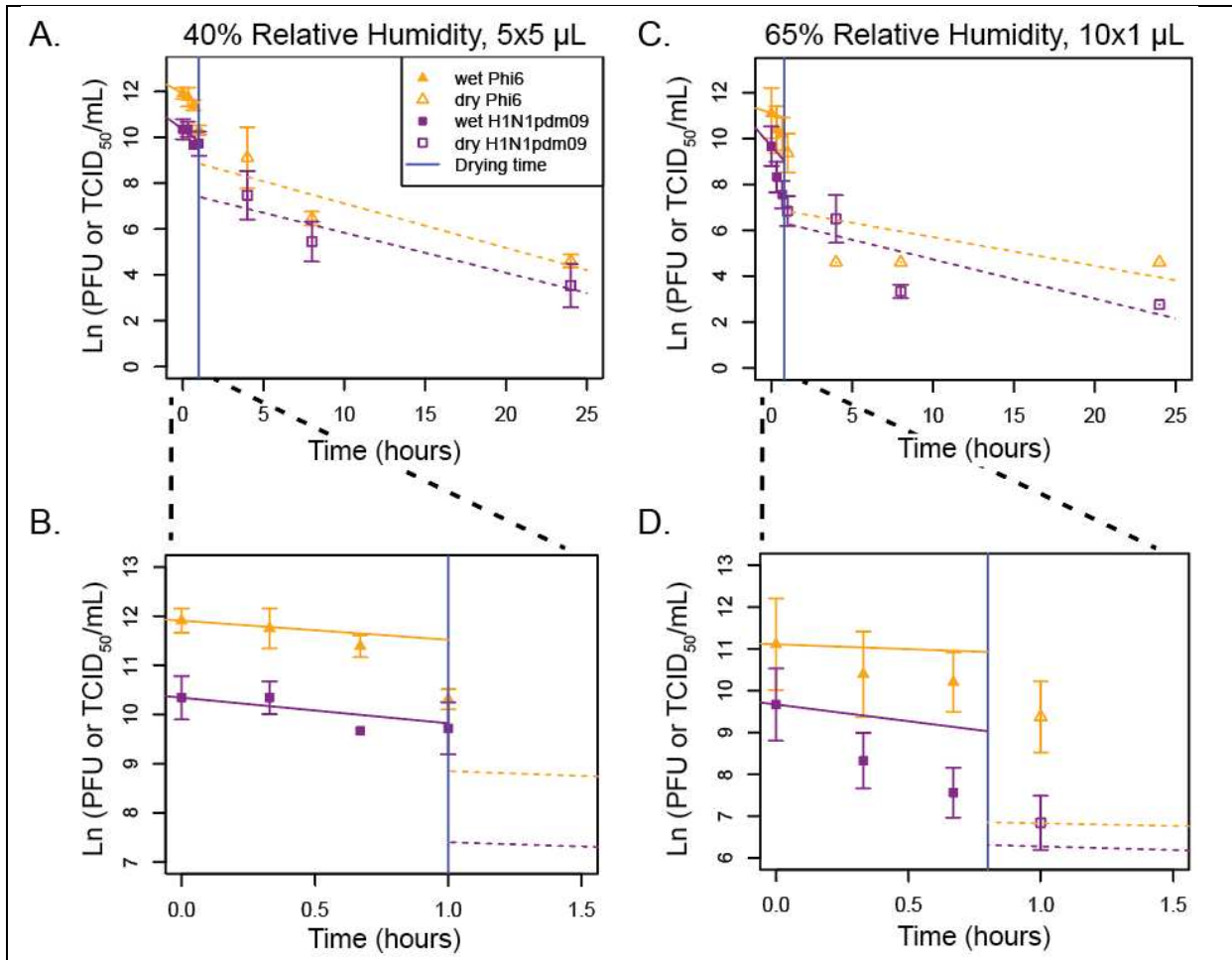


**Figure 3. Mechanistic first-order decay modeling of viral decay in 5x5  $\mu\text{L}$  droplets at 40% RH and 10x1  $\mu\text{L}$  droplets at 65% RH shows that viral decay during the wet phase is greater than decay during the dry phase.** A-D. First order exponential decay models, accounting for increasing solute concentrations over time during the wet phase, were fit to  $\ln(\text{PFU or TCID}_{50}/\text{mL})$  over time for (A-B) 5x5  $\mu\text{L}$  at 40% RH or (C-D) 10x1  $\mu\text{L}$  droplets at 65% RH. B,D A magnification of A,C from 0 to 1.5 hours is shown. For all graphs N=3 except at 1 hour where H1N1pdm09 N=6. The vertical blue line indicates the time of transition from the wet phase to the dry phase. A t-test was used to compare the slopes between the evaporation and dry phases for each virus at each droplet volume and between the phases for each virus at each droplet volume ( $p < 0.05$ ). Statistical details can be found in Supplemental Table 5.

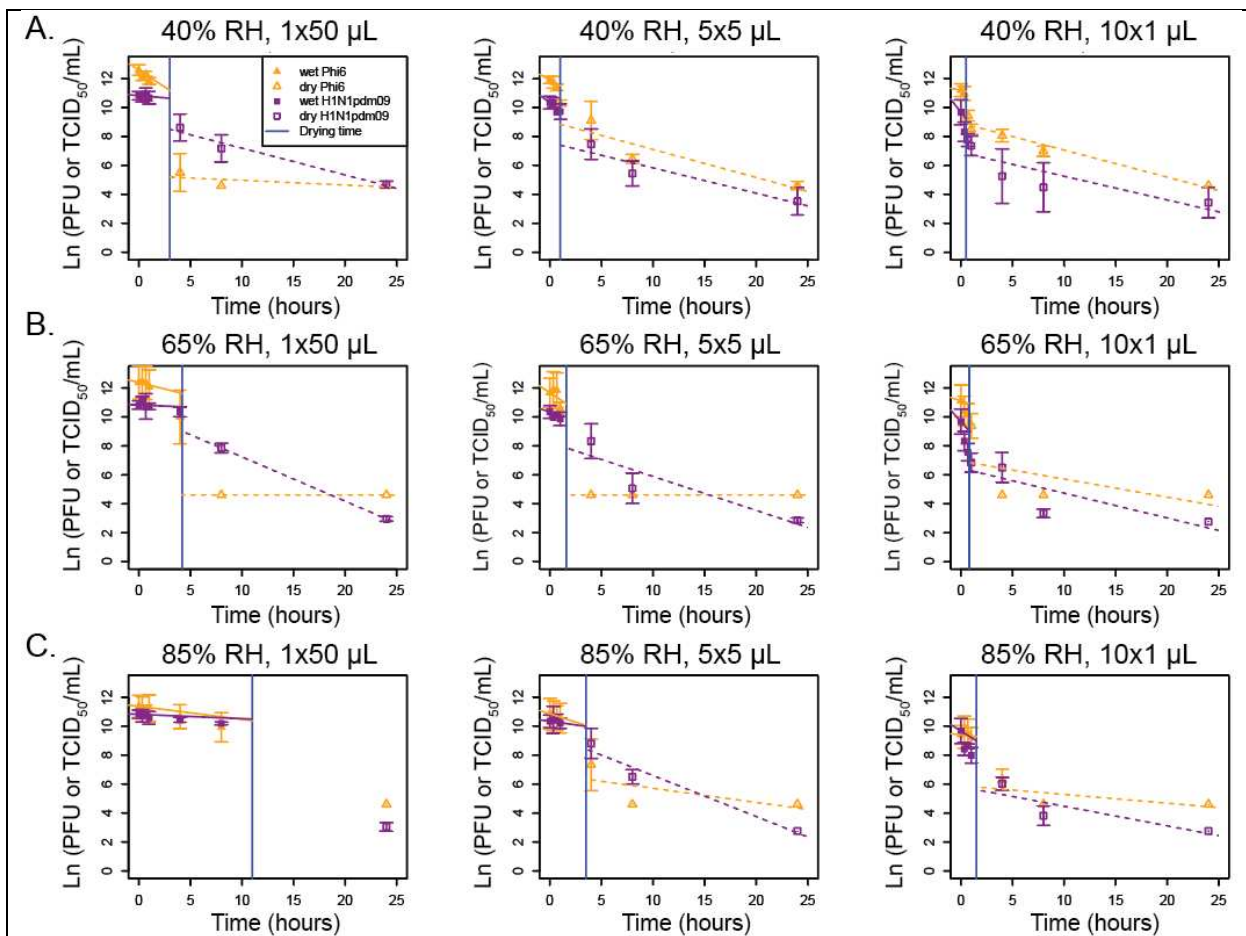


**Figure 4. Mechanistic, first-order exponential decay modeling shows that the decay during the wet phase is greater or similar to the rate of decay the dry phase.** A-C. First-order exponential decay models, accounting for increasing solute concentrations over time during the wet phase, were fit to  $\ln(\text{PFU or TCID}_{50}/\text{mL})$  over time for  $1 \times 50 \mu\text{L}$ ,  $5 \times 5 \mu\text{L}$ , or  $10 \times 1 \mu\text{L}$  droplets at (A) 40% RH, (B), 65% RH, (C) or 85% RH. For the wet phase, the fitted initial decay rate is shown. For all graphs  $N=3$  except at 1 hour where H1N1pdm09  $N=6$ . The vertical blue line indicates the time of transition from the wet phase to the dry phase. A t-test was used to compare the slopes between the evaporation and dry phases for each virus at each droplet volume and between the phases for each virus at each droplet volume ( $p < 0.05$ ). Statistical details can be found in Supplemental Table 5.

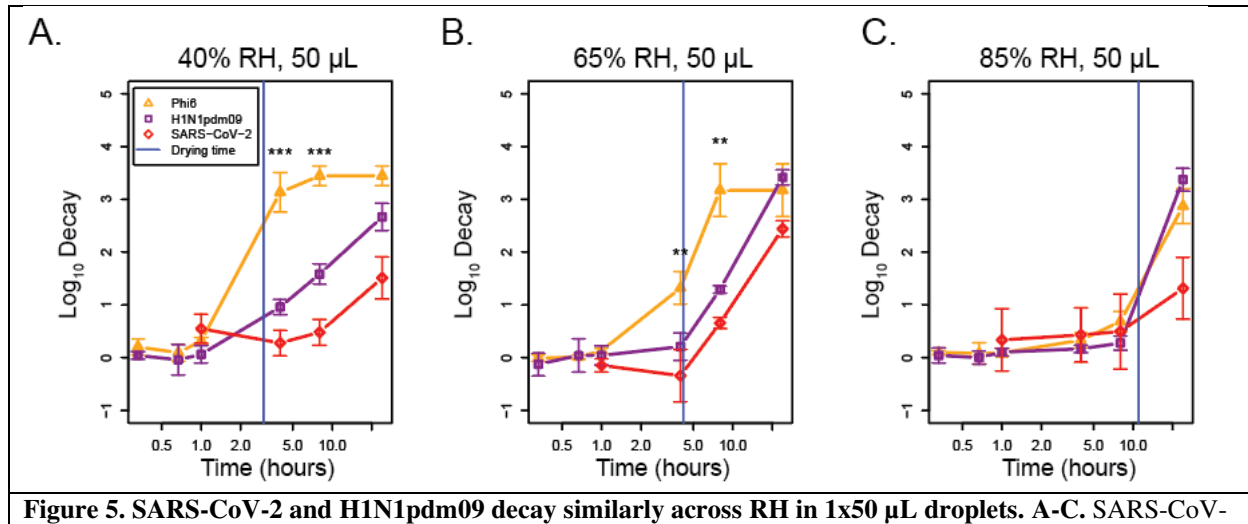


**Figure 5. SARS-CoV-2 and H1N1pdm09 decay similarly across RH in  $1\times 50\text{ }\mu\text{L}$  droplets.** A-C. SARS-CoV-2, H1N1pdm09, and Phi6 stability were measured at (A) 40%, (B) 65%, (C) and 85% RH in  $50\text{ }\mu\text{L}$  droplets using SARS-CoV-2 data originally published in Morris et al.<sup>2</sup> The vertical blue line indicates the time of transition from the wet phase to the dry phase. A one-way ANOVA and Tukey TSD test were used to determine statistical significance. Statistical details can be found in Supplemental Table 6.

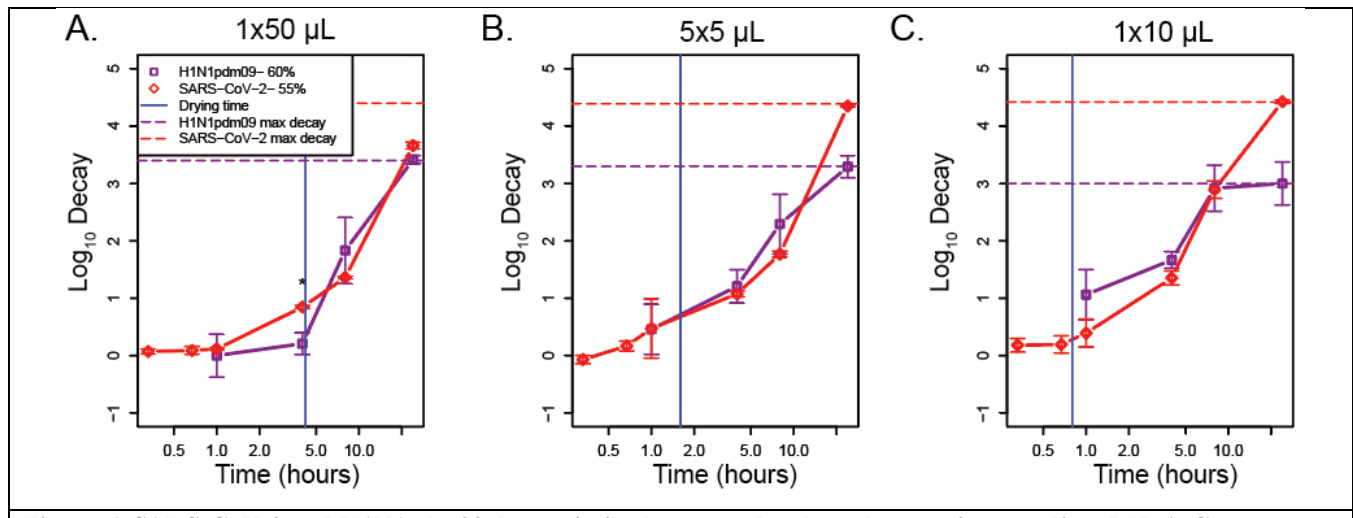


**Figure 6. SARS-CoV-2 and H1N1pdm09 decay similarly across droplet volume at intermediate RH.** A-C. SARS-CoV-2 stability was compared to H1N1pdm09 at 55-60% RH in  $1\times 50\text{ }\mu\text{L}$  (A),  $5\times 5\text{ }\mu\text{L}$  (B), and  $1\times 10\text{ }\mu\text{L}$  (C) droplets over time. The vertical blue line indicates the time of transition from the wet phase to the dry phase. A one-way ANOVA was used to determine statistical significance. Statistical details can be found in Supplemental Table 7.

RH (%)	Initial Volume (μL)	Exponential Decay Rate Constants ( $\frac{1}{\text{hour}}$ )			
		Phi6		H1N1pdm09	
		Wet Phase	Dry Phase	Wet Phase	Dry Phase
40	50	0·47 ± 0·23	0·03 ± 0·04 <sup>+</sup>	0·06 ± 0·13	0·19 ± 0·03 <sup>+</sup>
40	5	0·39 ± 0·02*	0·19 ± 0·09*	0·52 ± 0·16*	0·17 ± 0·06*
40	1	0·14 ± NA	0·19 ± 0·03	0·92 ± NA	0·16 ± 0·06
65	50	0·18 ± 0·01 <sup>+</sup>	<0·01 ± NA	0·03 ± 0·01 <sup>+</sup>	0·31 ± NA
65	5	0·47 ± 0·23*	<0·01 ± 0·00** <sup>+</sup>	0·23 ± 0·15	0·23 ± 0·11 <sup>+</sup>
65	1	0·23 ± 0·21	0·13 ± 0·14	0·80 ± 0·43	0·17 ± 0·08
85	50	0·09 ± 0·01 <sup>+</sup>	NA ± NA	0·03 ± 0·01 <sup>+</sup>	NA ± NA
85	5	0·23 ± 0·03	0·10 ± 0·11	0·10 ± 0·17	0·28 ± 0·06
85	1	0·08 ± 0·02	0·06 ± 0·07	0·45 ± 0·25	0·14 ± 0·08

NA indicates that a line could not be fit due to only 1 point occurring during the dry phase or that standard error could not be calculated due to having only 2 points to fit.

\* Significant difference in rate constant between the wet and dry phase for the given volume and virus.

<sup>+</sup> Significant difference between Phi6 and H1N1pdm09 for the given phase and volume.

**Table 1:** First-order exponential decay rate constants, adjusted for changing solute concentrations in the wet phase, for Phi6 and H1N1pdm09